THE JOURNAL OF PHYSICAL CHEMISTRY LETTERS
A JOURNAL OF THE AMERICAN CHEMICAL SOCIETY

pubs.acs.org/JPCL

Letter

Modeling Spin-Dependent Nonadiabatic Dynamics with Electronic Degeneracy: A Phase-Space Surface-Hopping Method

Xuezhi Bian, Yanze Wu, Jonathan Rawlinson, Robert G. Littlejohn, and Joseph E. Subotnik*

Cite This: J. Phys. Chem. Lett. 2022, 13, 7398−7404

Read Online

ACCESS | Metrics & More | Article Recommendations | Supporting Information

ABSTRACT: Nuclear Berry curvature effects emerge from electronic spin degeneracy and can lead to nontrivial spin-dependent (nonadiabatic) nuclear dynamics. However, such effects are not captured fully by any current mixed quantum-classical method such as fewest-switches surface hopping. In this work, we present a phase-space surface-hopping (PSSH) approach to simulate singlet−triplet intersystem crossing dynamics. We show that with a simple pseudodiabatic ansatz, a PSSH algorithm can capture the relevant Berry curvature effects and make predictions in agreement with exact quantum dynamics for a simple singlet−triplet model Hamiltonian. Thus, this approach represents an important step toward simulating photochemical and spin processes concomitantly, as relevant to intersystem crossing and spin−lattice relaxation dynamics.

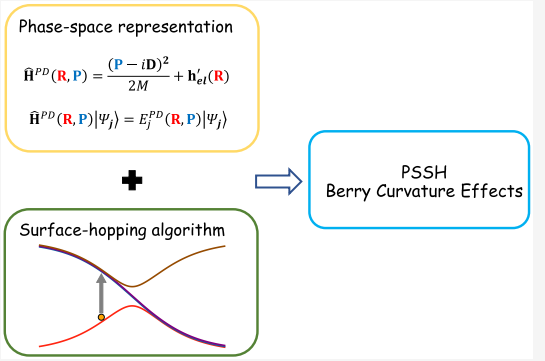

While not always fully appreciated, the spin degrees of freedom pertaining to a molecular or material system can be of particular importance when electronic transitions occur between states with different spin multiplicities (e.g., intersystem crossing [ISC]) or when states with large multiplicities interconvert (e.g., triplet internal conversion [IC]).[1,2] After all, nonadiabatic nuclear−electronic dynamics underlie many key phenomena in physical chemistry and chemical physics, including scattering,[3] charge transfer,[4] and photochemical processes,[5] and nontrivial spin degrees of freedom are almost always present. For instance, recent water (H_2O) splitting experiments have shown that if one can produce OH radicals of the same spin then one can effectively block H_2O_2 production and increase the yield of H_2 and O_2.[6] Currently, there are a wide range of mixed quantum-classical (MQC) methods[7−10] such as mean-field Ehrenfest dynamics (MFE),[11,12] fewest-switches surface hopping (FSSH),[13−15] and *ab initio* multiple spawning (AIMS)[16] for efficiently modeling *ab initio* nonadiabatic dynamics with reasonable accuracy, and many of these methods have been extended in principle to models of spin-crossover dynamics.[17−20] However, there are clear limitations to what physics these algorithms can capture. In particular, none of the algorithms above can model the effects of Berry curvature (and Berry force) in full generality.[21]

For the sake of completeness, a small introduction to Berry curvature would now appear to be appropriate. In principle, Berry curvature effects come in two flavors. The first flavor arises when a molecule with an even number of electrons is in a magnetic field and nuclear dynamics follow a single (adiabatic) electronic potential energy surface that is reasonably separated energetically from all other surfaces.[22−24] In such a case, as a result of non-Born−Oppenheimer derivative couplings to the other electronic adiabatic surfaces, the nuclei will experience a Lorentz-like force of the form

$$\mathbf{F}_j^{\mathrm{B}} = \boldsymbol{\Omega}_j \cdot \dot{\mathbf{R}} = (i\hbar\nabla \times \mathbf{d}_{jj}) \cdot \dot{\mathbf{R}} = \sum_k 2\hbar Im(\mathbf{d}_{jk} \cdot \dot{\mathbf{R}})\mathbf{d}_{kj} \tag{1}$$

Here $\mathbf{F}_j^{\mathrm{B}}$ and $\boldsymbol{\Omega}_j$ denote the Berry force and Berry curvature on surface j, $\dot{\mathbf{R}}$ is the nuclear velocity, and $\mathbf{d}_{jk}$ is the derivative coupling vector between adiabats $|\psi_j\rangle$ and $|\psi_k\rangle$. Note that when spin-related couplings (spin−orbit couplings [SOC],[25] spin−spin couplings,[26] magnetic fields,[27] etc.) are taken into account, the system Hamiltonian and the derivative coupling become complex-valued and the Berry force in eq 1 is nonzero (and can be large).[28]

The second flavor of Berry curvature is the full nonadiabatic tensor that arises when multiple states come together and there is a crossing. For instance, consider a system with a number of degenerate or nearly degenerate states crossing each other and one cannot separate the electronic manifold into a well-defined set of electronic states that interact in a fairly simple pairwise fashion; a common example would be an ISC event where a singlet crosses three triplets and all three triplets are deeply entangled and interact with the singlet.[21] In such a case, Berry curvature effects arise even if the Hamiltonian is real-valued (with the on-diagonal terms of the Berry curvature tensor

Received: June 10, 2022
Accepted: July 22, 2022
Published: August 4, 2022

being exactly zero). To our knowledge, effectively none of the quantum-classical schemes that are popularly used today (as propagated either in the adiabatic or diabatic representations) include such Berry curvature effects in their non-Born–Oppenheimer dynamics.

To that end, over the past few years, we have been working intensively to find a path to incorporate Berry curvature effects into the FSSH algorithm (for both the nondegenerate and degenerate cases).[29−31] Our algorithms (published in refs 29−31) were based on the premise of including Berry forces when propagating along a given adiabatic state in the usual FSSH framework. The final routine was able to perform fairly well on a variety of model Hamiltonians, but with two severe drawbacks: (i) the algorithms were very complicated and essentially *ad hoc* (beyond the usual assumptions/approximations/guesses inherent in FSSH[32,33]) and (ii) the algorithms were hard to implement in *ab initio* calculations. Recently, however, for the case of a nondegenerate problem, we proposed a novel, different ansatz: a pseudodiabatic phase space surface-hopping (PSSH) algorithm.[34] The basic premise of PSSH is to propagate nuclear motion along phase-space adiabats that naturally incorporate all pseudomagnetic field effects. PSSH reduces to FSSH without any spin degrees of freedom and is very simple to rationalize and implement in general. Moreover, in ref 34, numerical simulation showed that PSSH outperforms all FSSH-inspired algorithms for the case of a nondegenerate complex-valued model Hamiltonian when Berry forces are crucial.

With this background in mind, our goal in this letter is to extend the PSSH algorithm from ref 34 to a degenerate singlet−triplet ISC model. By comparison with exact data, we will show that the PSSH algorithm can capture Berry curvature effects nearly quantitatively for an interesting model Hamiltonian, outperforming the algorithm published in ref 31 and with a very simple and generalized algorithm. As such, in the future, we believe the present algorithm will be the optimal protocol for simulating spin-dependent nonadiabatic dynamics with electronic degeneracy. As a side note, we are also hopeful that the phase-space formulation introduced below can also provide some insights into other MQC methods such as MFE and AIMS.

Before concluding this introduction, we emphasize that developing tools to study nonadiabatic transitions with spin degrees of freedom is very important in making progress on one of the most exciting themes today in physical chemistry: the chiral induced spin selectivity (CISS) effect.[35,36] Recent experiments have demonstrated that when a current passes through a chiral molecule, that current is often very spin-polarized, and this spin polarization can increase as temperature increases.[37] Thus, understanding nuclear dynamics in the presence of both spin and electronic degrees of freedom would be crucial for developing a comprehensive model of the CISS effect.[38−42]

METHOD

To introduce the PSSH algorithm, let us consider a reasonably generic singlet−triplet ISC Hamiltonian in a spin-diabatic basis of the form $\hat{\mathbf{H}} = \hat{\mathbf{P}}^2/2M + \hat{\mathbf{h}}_{el}(\hat{\mathbf{R}})$ with an electronic Hamiltonian:

$$\hat{\mathbf{h}}_{el}(\hat{\mathbf{R}}) = \begin{pmatrix} \epsilon_S & V & Ve^{i\phi} & Ve^{-i\phi} \\ V & \epsilon_T & 0 & 0 \\ Ve^{-i\phi} & 0 & \epsilon_T & 0 \\ Ve^{i\phi} & 0 & 0 & \epsilon_T \end{pmatrix} \tag{2}$$

The singlet spin diabat $|S\rangle$ with energy ϵ_S crosses with three triplet spin diabats $|T_0\rangle$, $|T_1\rangle$, and $|T_{-1}\rangle$ with energy ϵ_T and couples with triplets through SOCs with different phases. Here, (i) the diabatic energies ϵ_S and ϵ_T, (ii) the coupling strength V, and (iii) the variable ϕ that modulates the complex phase of the SOC are all real-valued and vary with nuclear coordinates $\hat{\mathbf{R}}$. One would like to simulate nonadiabatic dynamics with such a Hamiltonian while taking into account the fact that $\nabla\phi \neq 0$.

According to PSSH, we apply a basis transformation to cancel the complex-valued phases on the couplings

$$\hat{\mathbf{h}}'_{el}(\hat{\mathbf{R}}) = \mathbf{\Lambda}^\dagger \hat{\mathbf{h}}_{el}(\hat{\mathbf{R}})\mathbf{\Lambda} = \begin{pmatrix} \epsilon_S & V & V & V \\ V & \epsilon_T & 0 & 0 \\ V & 0 & \epsilon_T & 0 \\ V & 0 & 0 & \epsilon_T \end{pmatrix} \tag{3}$$

where the transformation matrix reads

$$\mathbf{\Lambda} = \begin{pmatrix} 1 & 0 & 0 & 0 \\ 0 & 1 & 0 & 0 \\ 0 & 0 & e^{-i\phi} & 0 \\ 0 & 0 & 0 & e^{i\phi} \end{pmatrix} \tag{4}$$

In this new basis, the Hamiltonian is now real-valued and the absolute values of the coupling matrix elements are not changed. Note, however, that the basis in eq 3 is no longer diabatic because the electronic states depend on the nuclear coordinates (and so a derivative coupling must emerge). Henceforth, we will refer to this new basis as the "pseudodiabatic" basis. The total effective Hamiltonian within the pseudodiabatic basis then becomes

$$\hat{\mathbf{H}}^{PD}(\mathbf{R}, \mathbf{P}) = \frac{(\hat{\mathbf{P}} - i\hbar\hat{\mathbf{D}}(\hat{\mathbf{R}}))^2}{2M} + \hat{\mathbf{h}}'_{el}(\hat{\mathbf{R}}) \tag{5}$$

where $\hat{\mathbf{D}} = \Lambda^\dagger\nabla\Lambda$ is the derivative coupling operator between pseudodiabats (we use $\hat{\mathbf{D}}$ to distinguish this derivative coupling from the derivative coupling $\hat{\mathbf{d}}$ between adiabats). In matrix form,

$$\hat{\mathbf{D}} = \begin{pmatrix} 0 & 0 & 0 & 0 \\ 0 & 0 & 0 & 0 \\ 0 & 0 & -i\nabla\phi & 0 \\ 0 & 0 & 0 & i\nabla\phi \end{pmatrix} \tag{6}$$

At this point, according to PSSH, we apply a Wigner transform to map the quantum mechanical nuclear operators $\hat{\mathbf{R}}$ and $\hat{\mathbf{P}}$ to classical variables $\mathbf{R}$ and $\mathbf{P}$. Thereafter, we diagonalize the total phase-space Hamiltonian $\hat{\mathbf{H}}^{PD}(\mathbf{R}, \mathbf{P})$ in eq 5, and we define a new eigenbasis of "phase-space adiabats" labeled by $\{|\Psi_j^{PD}\rangle\}$ with eigenenergy E_j^{PD}:

$$\hat{\mathbf{H}}^{PD}(\mathbf{R}, \mathbf{P})|\Psi_j^{PD}\rangle = E_j^{PD}(\mathbf{R}, \mathbf{P})|\Psi_j^{PD}\rangle \tag{7}$$

https://doi.org/10.1021/acs.jpclett.2c01802
J. Phys. Chem. Lett. 2022, 13, 7398−7404

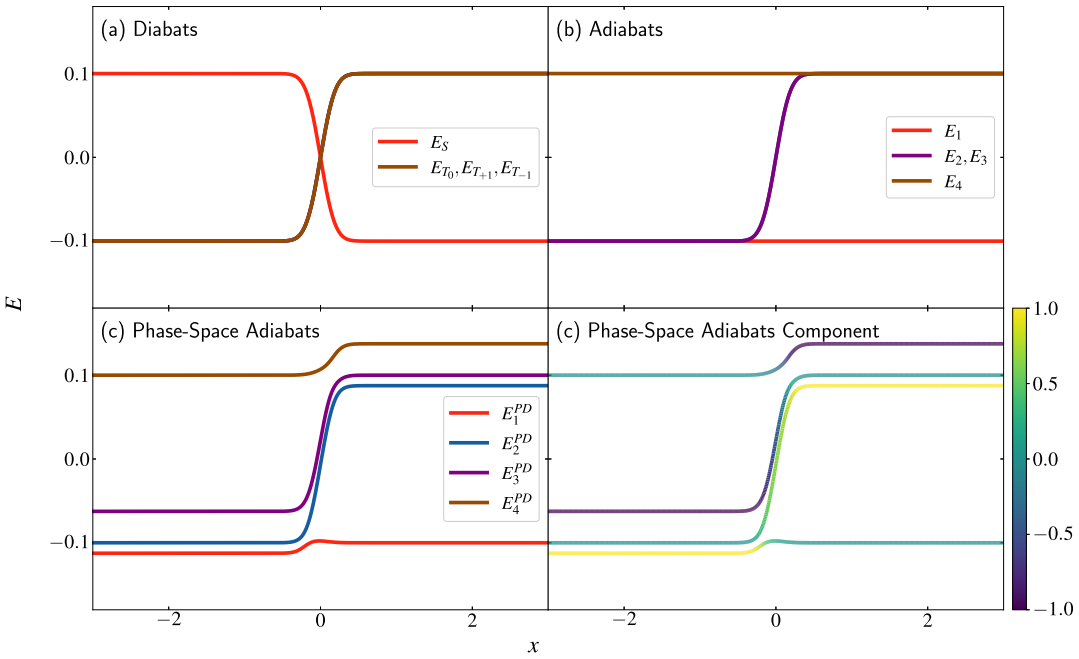

Figure 1. (a) Diabatic, (b) adiabatic, and (c) pseudodiabatic (PD) phase-space adiabatic potential energy surfaces (PESs) for the singlet−triplet crossing Hamiltonian described in eq 15 as a function of nuclear coordinate x. The phase-space adiabats are calculated for the case $P_y^{\text{can}} = 5.0$. Note that, for this Hamiltonian, P_y^{can} is actually a constant of the motion. (d) The color map indicates the spin character $\eta = \langle \Psi_j^{\text{PD}} | \hat{\sigma}_z | \Psi_j^{\text{PD}} \rangle$ of all of the phase-space adiabats. For instance, when $\eta = 1$, the phase-space adiabat is effectively the $|T_1\rangle$ triplet; when $\eta = -1$, the phase-space adiabat is effectively the $|T_{-1}\rangle$ triplet. This color map allows one to assign the spin state heuristically to each phase-space adiabat. Asymptotically, the phase-space adiabats have a one-to-one mapping to the spin diabats.

Two points about nomenclature are worth mentioning. First, phase-space adiabats are analogous to the normal position-space adiabats that are obtained from diagonalizing the electronic Hamiltonian $\hat{\mathbf{h}}_{\text{el}}(\mathbf{R})$ in a diabatic basis. For a real-valued Hamiltonian, one can easily see that the pseudodiabatic derivative coupling matrix $\hat{\mathbf{D}}$ will be zero and the phase-space adiabats will be identical to the normal position-space adiabats. Second, the phase-space adiabats introduced above are not equivalent to the superadiabats as proposed by Shenvi,[43] the latter of which are obtained from diagonalizing the phase-space Hamiltonian $\hat{\mathbf{H}}^{\text{PS}}$ in the adiabatic basis where $\mathbf{H}_{jk}^{\text{PS}} = (\mathbf{P}\delta_{jk} - i\hbar\mathbf{d}_{jk})^2/2M + E_j\delta_{jk}$. The eigenvalues and eigenvectors of both $\mathbf{H}^{\text{PD}}$ and $\mathbf{H}^{\text{PS}}$ will depend on $\mathbf{R}$ and $\mathbf{P}$, but they will not be the same.

With the background above in mind, we will now outline the PSSH algorithm as appropriate for an ISC event. As inspired by Shenvi's PSSH and following the spirit of Tully's FSSH, the algorithm starts from sampling a swarm of independent trajectories with a random $\mathbf{R}$ and $\mathbf{P}$ so as to sample the Wigner distribution for a quantum wavepacket. Each trajectory carries a phase-space quantum amplitude $\mathbf{c}$ and a phase-space adiabat label n that is determined by $\mathbf{c}$. Note that the classical momentum sampled from a quantum wavepacket in a diabatic basis is equivalent to the kinetic momentum $\mathbf{P}^{\text{kinetic}} = M\dot{\mathbf{R}}$. However, PSSH propagates the canonical momentum $\mathbf{P}_n$ (rather than the kinetic momentum). When working within a pseudodiabatic basis defined by eq 4, the correct relationship between the kinetic and canonical momenta is

$$\mathbf{P}_n = \mathbf{P}_n^{\text{kinetic}} + i\hbar\mathbf{D}_{nn} \tag{8}$$

At this point, in the spirit of both Hamilton's equations and Tully's algorithm, according to PSSH, the classical variables $\mathbf{R}$ and $\mathbf{P}$ of each trajectory are propagated along a single active phase-space adiabat n according to

$$\dot{\mathbf{R}} = \nabla_{\mathbf{P}} E_n^{\text{PD}} = \langle \Psi_n^{\text{PD}} | \nabla_{\mathbf{P}} \hat{\mathbf{H}}^{\text{PD}} | \Psi_n^{\text{PD}} \rangle \tag{9}$$

$$\dot{\mathbf{P}} = -\nabla_{\mathbf{R}} E_n^{\text{PD}} = -\langle \Psi_n^{\text{PD}} | \nabla_{\mathbf{R}} \hat{\mathbf{H}}^{\text{PD}} | \Psi_n^{\text{PD}} \rangle \tag{10}$$

The electronic part is treated quantum mechanically and integrated by the Schrödinger equation

$$\dot{c}_n = -\frac{i}{\hbar} E_n^{\text{PD}} c_n - \sum_k T_{nk} c_k \tag{11}$$

where the time derivative coupling matrix $\mathbf{T}$ can be calculated from the matrix log of the overlap:[44]

$$T_{nk} = \left\langle \Psi_n \middle| \frac{d\Psi_k}{dt} \right\rangle = \frac{[\log(\mathbf{U})]_{nk}}{\Delta t} \tag{12}$$

Here, the overlap matrix $\mathbf{U}$ is defined by $U_{nk} = \langle \Psi_n(t) | \Psi_k(t + \Delta t) \rangle$ and Δt is the length of the discrete time step in the simulation.

At each time step, the trajectory on active phase-space adiabat n has the chance to hop to another phase-space adiabat k with probability

$$g_{n\to k} = \max\left[2\Delta t Re\left(T_{nk} \frac{\rho_{kn}}{\rho_{nn}} \right), 0 \right] \tag{13}$$

where the electronic density matrix elements are $\rho_{kn} = c_k c_n^*$. After a successful hop from state n to state k, the trajectory rescales its momentum along the direction of the position component of the derivative coupling $\mathbf{d}_{nk}^{\text{R,PD}}$ between phase-space adiabats n and k to conserve energy, where

https://doi.org/10.1021/acs.jpclett.2c01802
J. Phys. Chem. Lett. 2022, 13, 7398−7404

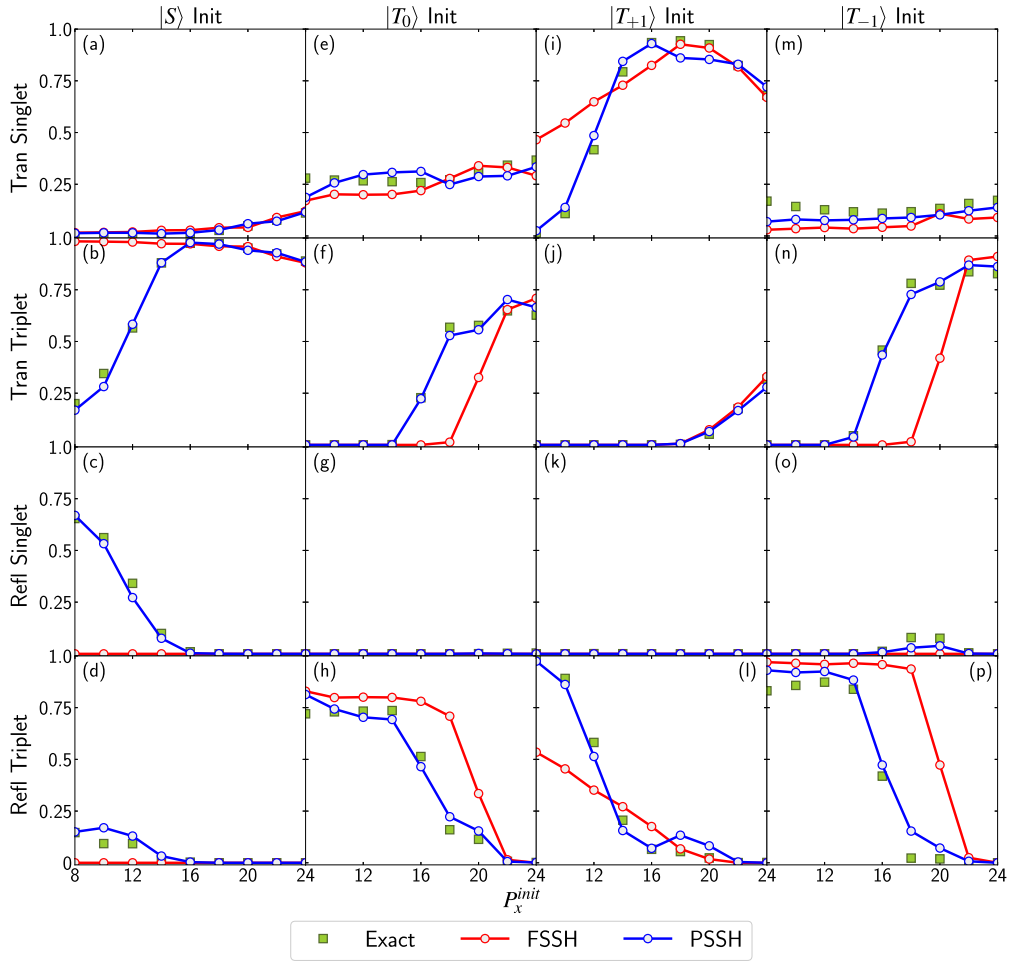

Figure 2. Results for transmission and reflection populations according to exact dynamics, standard surface hopping, and phase-space surface-hopping algorithms. The systems are initialized on (a–d) the singlet spin diabat $|S\rangle$, (e–h) the triplet $|T_0\rangle$, (i–l) the triplet $|T_{+1}\rangle$, and (m–p) the triplet $|T_{-1}\rangle$. The PSSH method shows strong agreement with the exact results, whereas standard FSSH often is very incorrect.

$$\mathbf{d}_{nk}^{\mathbf{R},\mathrm{PD}} = \langle \Psi_n | \nabla_{\mathbf{R}} | \Psi_k \rangle = \frac{\langle \Psi_n | \nabla_{\mathbf{R}} \hat{\mathbf{H}}^{\mathrm{PD}} | \Psi_k \rangle}{E_k^{\mathrm{PD}} - E_n^{\mathrm{PD}}} \tag{14}$$

Note that in a phase-space formulation, the derivative coupling also has a momentum component $\mathbf{d}_{\mathrm{nk}}^{\mathbf{P},\mathrm{PD}} = \langle \Psi_n | \nabla_{\mathbf{P}} | \Psi_k \rangle = \frac{\langle \Psi_n | \nabla_{\mathbf{P}} \hat{\mathbf{H}}^{\mathrm{PD}} | \Psi_k \rangle}{E_k^{\mathrm{PD}} - E_n^{\mathrm{PD}}}$. In general, one can imagine rescaling both momenta and position at the time of a hop, but we do not consider such an "optimal"[45] hop for simple reasons of computational feasibility.[43]

In practice, to satisfy energy conservation, one must search numerically along the direction $\mathbf{d}_{nk}^{\mathbf{R},\mathrm{PD}}$ when rescaling the momentum because the kinetic energy and potential energy cannot be separated within a phase-space representation; that being said, the energy function is still quadratic in momentum so that one simply picks the closest energy-conserving solution.

The description above summarizes the salient features of the PSSH algorithm as compared with FSSH; all other PSSH details are identical to the FSSH details. We will now show numerically that this scheme gives a very accurate treatment of ISC dynamics.

Over the past few years, we have diligently attempted to derive a surface-hopping ansatz to propagate the dynamics for the following model Hamiltonian mimicking a simple singlet–triplet crossing:

$$\hat{\mathbf{h}}_{\mathrm{el}} = A \begin{pmatrix} \cos\theta & \frac{1}{\sqrt{3}}\sin\theta & \frac{1}{\sqrt{3}}\sin\theta e^{i\phi} & \frac{1}{\sqrt{3}}\sin\theta e^{-i\phi} \\ \frac{1}{\sqrt{3}}\sin\theta & -\cos\theta & 0 & 0 \\ \frac{1}{\sqrt{3}}\sin\theta e^{-i\phi} & 0 & -\cos\theta & 0 \\ \frac{1}{\sqrt{3}}\sin\theta e^{i\phi} & 0 & 0 & -\cos\theta \end{pmatrix} \tag{15}$$

Here we define $\theta \equiv \frac{\pi}{2}(\mathrm{erf}(Bx) + 1)$ and $\phi \equiv Wy$, and we set $A = 0.10$, $B = 3.0$, and $W = 5.0$ as constants.

In Figure 1, we show a schematic plot of the diabats and adiabats. The three triplet diabats are degenerate over all space and cross with the singlet diabat at $x = 0$ (Figure 1(a)). The smallest and largest adiabats E_1 and E_4 are also flat in the x direction, and two degenerate adiabats E_2 and E_3 connect them in the middle (Figure 1(b)). The topology of the diabatic and adiabatic PESs is extremely simple for this Hamiltonian.

Now if one performs a calculation, it is fairly straightforward to observe that, for this problem, the pseudodiabatic derivative coupling is simply $\hat{D}_x = 0$ and $\hat{D}_y = \mathrm{diag}(0 \;\; 0 \;\; W \;\; -W)$. Thus, one can calculate phase-space adiabats as functions of nuclear coordinate x (as they are all completely flat in the y direction for the given Hamiltonian in eq 15) and P_y. In Figure

https://doi.org/10.1021/acs.jpclett.2c01802
J. Phys. Chem. Lett. 2022, 13, 7398–7404

1(c), we plot the phase-space adiabats with $P_y = W$. Several interesting features arise, upon which we will now elaborate.

First, notice that the color map of the spin characteristics of the phase-space adiabats (as calculated in Figure 1(d) by calculating $\langle \Psi_j^{PD} | \hat{\sigma}_z | \Psi_j^{PD} \rangle$) shows that this problem is really a complicated crossing of many states with no two-state analogue. This is a topologically nontrivial crossing, and the topology of the phase-space adiabats can be very different if one changes P_y.

Second, note that the degeneracy of the three adiabats is lifted in phase space when $x \to \pm\infty$. The three phase-space adiabats have a one-to-one mapping with three triplet diabats asymptotically given the fact that $V \to 0$ as $x \to \pm\infty$ and the total Hamiltonian matrix in eq 5 is diagonal. For instance, when $x \to \infty$, $|\Psi_3^{PD}\rangle$ should map to $|T_0\rangle$, and $|\Psi_2^{PD}\rangle$, $|\Psi_4^{PD}\rangle$ should map to $|T_{+1}\rangle$, $|T_{-1}\rangle$ correspondingly. This mapping and breaking of degeneracy is also made clear by Figure 1(d).

Third, consider an incoming trajectory on the singlet diabat $|S\rangle$ from the left with $\mathbf{P} = (P_x, P_y)$ and assume that $P_y > 0$. In phase space, the asymptotic energy barrier to transmit to the right on the upper surfaces should be increased by $(2P_yW + W^2)/2M$ on $|\Psi_4^{PD}\rangle$ (or $|T_{-1}\rangle$) and decreased by $(-2P_yW + W^2)/2M$ on $|\Psi_2^{PD}\rangle$ (or $|T_{+1}\rangle$). Thus, for the transmitting trajectories, one of the real physical observables—the kinetic momentum $\mathbf{P}^{kinetic}$—will be very different according to eq 8 for trajectories emerging on different phase-space adiabats; i.e., the nuclear motion will bend in different directions depending on the corresponding electronic state. Intuitively, without running any PSSH simulations, these three facts can explain a lot of the exotic bending and bifurcation phenomena summarized in Table 1 in ref 31.

To quantitatively assess the performance of the present PSSH algorithm, we have simulated scattering dynamics for the Hamiltonian in eq 15 and compared the results for transmission and reflection probabilities according to both exact wavepacket dynamics and Tully's standard FSSH algorithm. For the wavepacket dynamics, the system is initialized as a Gaussian wavepacket with the form

$$|\Psi_0(\mathbf{R})\rangle = \exp\left(-\frac{(\mathbf{R}-\mathbf{R}_0)^2}{\sigma^2} + \frac{i}{\hbar}\mathbf{P}_0\cdot\mathbf{R}\right)|\phi_i\rangle \tag{16}$$

We set the initial position $\mathbf{R}_0 = (-4, 0)$, the wavepacket width is set to $\sigma_x = \sigma_y = 1$, and the nuclear mass is $M = 1000$. We chose an initial momentum $\mathbf{P}_0 = (P_x^{init}, P_y^{init})$ with $P_x^{init} = P_y^{init}$, and we scan over the range of $P_x^{init} = 8-24$; all parameters are in atomic units. The initial wavepacket is set to be on one of the pure spin diabats. Exact wavepacket dynamics are propagated on a 2D grid by the split-operator method with the fast Fourier transform algorithm.[46] For the PSSH data, all results were generated following the method described above. The initial active phase-space adiabat of each trajectory was randomly assigned according to the quantum amplitude in the phase-space adiabatic basis. For PSSH, no velocity reversal (upon a frustrated hop) was implemented; for standard FSSH results, a velocity reversal was administered in the spirit of Truhlar's "∇V" approach.[47] (We also computed results for Tully's FSSH algorithm without any velocity reversal, and the results were equally disappointing.)

For both surface-hopping methods, 2×10^3 trajectories were sampled according to the Wigner distribution of eq 16.

Simulation results are presented in Figure 2. We find that Berry curvature effects lead to a change in the effective energy barrier for transmission on the different surfaces. For instance, according to exact wavepacket dynamics, a large population is reflected for the case in which the system begins on the upper singlet at low momentum ($P_x^{init} < 16$) (Figure 2(a–d)). Such a reflection is completely missing from the standard FSSH method. Similarly, for the cases in which dynamics begin on a lower triplet, the energy barrier for transmission is altered by the Berry curvature. The standard FSSH routinely predicts qualitatively wrong results, and the pseudodiabatic PSSH method matches the exact results almost quantitatively in all cases (as well as and usually better than the algorithm presented in ref 31). Clearly, the PSSH algorithm outperforms the standard FSSH algorithm in all cases because the FSSH algorithm completely neglects the contribution of Berry curvature effects, whereas the PSSH includes such effects explicitly. More results for systems beginning with different initial conditions can be found in the Supporting Information.

The strong results above have been achieved following a simple surface-hopping protocol (as opposed to the approach in ref 31) and make it clear that, if possible, a pseudodiabatic PSSH formulation is the best protocol for incorporating Berry curvature effects into spin-dependent MQC dynamics. With that being said, the algorithm described above is still not yet fully tested; beyond connecting the algorithm to more rigorous theories of nonadidabatic dynamics,[48,49] several practical points must be explored before we can begin running first-principles simulations.

The first and most important question that must be addressed is the question of how to choose a basis for the PSSH pseudodiabats. After all, for any Hamiltonian, there is no one fixed (unique) diabatic basis. For instance, we have constructed the Hamiltonian in eq 2 in an arbitrary laboratory frame with fixed x, y, and z directions; if one were to apply a fixed global change of the basis matrix and then boost the basis functions for the final Hamiltonian, then one would arrive at a different set of pseudodiabats (and therefore different PSSH dynamics). Vice versa, given the fact that one can change the basis to render the entire Hamiltonian in eq 2 real-valued,[50] one might also conclude that there is no reason to choose pseudodiabats that differ from true diabats and therefore PSSH dynamics would be exactly equivalent to FSSH dynamics. In short, the present PSSH algorithm sorely depends on the choice of diabats, and in the future, it will be essential to pick a good diabatic starting frame. The essential features of this frame are not yet known, but judging from the model presented here, ideally one would like a frame for which the norms of the derivative of SOC matrix elements ($|\nabla H_{SOC}|$) are small.

Second, so far we have considered an isolated singlet–triplet crossing. In the presence of an external magnetic field $\mathbf{B}$, the electronic Hamiltonian will break some of the degeneracy through the Zeeman interaction:

$$\hat{\mathbf{h}}_{el}(\hat{\mathbf{R}}) = \begin{pmatrix} \epsilon_S & V & Ve^{i\phi} & Ve^{-i\phi} \\ V & \epsilon_T & B_x - iB_y & B_x + iB_y \\ Ve^{-i\phi} & B_x + iB_y & \epsilon_T + B_z & 0 \\ Ve^{i\phi} & B_x - iB_y & 0 & \epsilon_T - B_z \end{pmatrix} \tag{17}$$

In such a case, one must ask, what is the correct basis for boosting the electronic frame and running PSSH? The answer may not appear to be obvious, but one path forward would be

https://doi.org/10.1021/acs.jpclett.2c01802
J. Phys. Chem. Lett. 2022, 13, 7398–7404

to orient the basis functions so that $\hat{z}$ is collinear with **B** (so that $B_x = B_y = 0$). In such a case, the problem is rendered completely equivalent to the problem above. Thus, if one can, in general, define an optimal basis for the singlet−triplet problem without a magnetic field present, then one can also likely construct an optimal basis for the singlet−triplet problem with a magnetic field present.

Third, simulating spin-dependent nonadiabatic nuclear−electronic dynamics in the condensed phases raises a host of questions that must be addressed. In a previous study using nonequilibrium Fermi's golden rule,[51] we found that spin polarization survived for some transient period of time for a simple spin-boson model with complex-valued coupling. In the future, it will be important to test whether the PSSH algorithm can recover such transient effects in complicated environments with friction; it will also be important to explore if and how PSSH recovers the detailed balance in the condensed phase. Finally, the question of decoherence[52,53] within the PSSH algorithm must be related to the ever-fascinating question of spin−lattice relaxation, which again gives us a strong motivation to further explore spin-dependent nonadiabatic dynamics with a surface-hopping formalism.

In conclusion, we have proposed a simple and general pseudodiabatic phase-space surface-hopping method for simulating spin-dependent nonadiabatic dynamics with electronic degeneracy as relevant to singlet−triplet ISC dynamics. For a simple model system, the algorithm shows significant improvements over the standard position-space surface hopping and captures Berry curvature effects while keeping the spirit of Tully's original FSSH algorithm (and Shenvi's insight into superadiabats[43]). Looking forward, there are a host of intriguing chemical reactions that can be altered by magnetic fields.[54] Given the fact that the nuclear Berry curvature usually acts like a pseudomagnetic field, it is likely that nuclear Berry curvature effects may be paramount in such magnetic chemical systems as well. Furthermore, there are a myriad of photochemical problems occurring in triplet states where ISC plays a key role.[55,56] We are hopeful that this method (and variants thereof) will soon be applied to model such systems with *ab initio* electronic structure.

■ ASSOCIATED CONTENT

Supporting Information

The Supporting Information is available free of charge at https://pubs.acs.org/doi/10.1021/acs.jpclett.2c01802.

Additional numerical results, including several different Hamiltonian parameters with different initial conditions; comparison between the current PSSH method versus FSSH and the quasi-diabatic Berry force method in ref 31 (PDF)

■ AUTHOR INFORMATION

Corresponding Author

Joseph E. Subotnik − *Department of Chemistry, University of Pennsylvania, Philadelphia, Pennsylvania 19104, United States*; Email: subotnik@sas.upenn.edu

Authors

Xuezhi Bian − *Department of Chemistry, University of Pennsylvania, Philadelphia, Pennsylvania 19104, United States*; orcid.org/0000-0001-6445-7462

Yanze Wu − *Department of Chemistry, University of Pennsylvania, Philadelphia, Pennsylvania 19104, United States*; orcid.org/0000-0001-9140-2782

Jonathan Rawlinson − *Department of Mathematics, University of Manchester, Manchester M13 9PL, U.K.*

Robert G. Littlejohn − *Department of Physics, University of California, Berkeley, California 94720, United States*

Complete contact information is available at: https://pubs.acs.org/10.1021/acs.jpclett.2c01802

Notes

The authors declare no competing financial interest.

■ ACKNOWLEDGMENTS

This material is based on work supported by the National Science Foundation under grant no. CHE-2102402.

■ REFERENCES

(1) Kasha, M. Characterization of electronic transitions in complex molecules. *Discuss. Faraday Soc.* **1950**, *9*, 14−19.

(2) Penfold, T. J.; Gindensperger, E.; Daniel, C.; Marian, C. M. Spin-vibronic mechanism for intersystem crossing. *Chem. Rev.* **2018**, *118*, 6975−7025.

(3) Shenvi, N.; Roy, S.; Tully, J. C. Dynamical steering and electronic excitation in NO scattering from a gold surface. *Science* **2009**, *326*, 829−832.

(4) Akimov, A. V.; Neukirch, A. J.; Prezhdo, O. V. Theoretical insights into photoinduced charge transfer and catalysis at oxide interfaces. *Chem. Rev.* **2013**, *113*, 4496−4565.

(5) Nelson, T. R.; White, A. J.; Bjorgaard, J. A.; Sifain, A. E.; Zhang, Y.; Nebgen, B.; Fernandez-Alberti, S.; Mozyrsky, D.; Roitberg, A. E.; Tretiak, S. Non-adiabatic excited-state molecular dynamics: Theory and applications for modeling photophysics in extended molecular materials. *Chem. Rev.* **2020**, *120*, 2215−2287.

(6) Ghosh, S.; Bloom, B. P.; Lu, Y.; Lamont, D.; Waldeck, D. H. Increasing the efficiency of water splitting through spin polarization using cobalt oxide thin film catalysts. *J. Phys. Chem. C* **2020**, *124*, 22610−22618.

(7) Agostini, F.; Curchod, B. F. Different flavors of nonadiabatic molecular dynamics. *WIREs Comput. Mol. Sci.* **2019**, *9*, e1417.

(8) Crespo-Otero, R.; Barbatti, M. Recent advances and perspectives on nonadiabatic mixed quantum-classical dynamics. *Chem. Rev.* **2018**, *118*, 7026−7068.

(9) Coker, D. F.; Xiao, L. Methods for molecular dynamics with nonadiabatic transitions. *J. Chem. Phys.* **1995**, *102*, 496−510.

(10) Tully, J. Mixed quantum-classical dynamics. *Faraday Discuss.* **1998**, *110*, 407−419.

(11) Bedard-Hearn, M. J.; Larsen, R. E.; Schwartz, B. J. Mean-field dynamics with stochastic decoherence (MF-SD): A new algorithm for nonadiabatic mixed quantum/classical molecular-dynamics simulations with nuclear-induced decoherence. *J. Chem. Phys.* **2005**, *123*, 234106.

(12) Cotton, S. J.; Miller, W. H. Symmetrical windowing for quantum states in quasi-classical trajectory simulations. *J. Phys. Chem. A* **2013**, *117*, 7190−7194.

(13) Tully, J. C. Molecular dynamics with electronic transitions. *J. Chem. Phys.* **1990**, *93*, 1061−1071.

(14) Wang, L.; Akimov, A.; Prezhdo, O. V. Recent progress in surface hopping: 2011−2015. *J. Phys. Chem. Lett.* **2016**, *7*, 2100−2112.

(15) Subotnik, J. E.; Jain, A.; Landry, B.; Petit, A.; Ouyang, W.; Bellonzi, N. Understanding the surface hopping view of electronic transitions and decoherence. *Annu. Rev. Phys. Chem.* **2016**, *67*, 387−417.

(16) Ben-Nun, M.; Quenneville, J.; Martínez, T. J. Ab initio multiple spawning: Photochemistry from first principles quantum molecular dynamics. *J. Phys. Chem. A* **2000**, *104*, 5161−5175.

(17) Mukherjee, S.; Fedorov, D. A.; Varganov, S. A. Modeling Spin-Crossover Dynamics. *Annu. Rev. Phys. Chem.* **2021**, *72*, 515−540.
(18) Mai, S.; Marquetand, P.; González, L. A general method to describe intersystem crossing dynamics in trajectory surface hopping. *InterNatl. J. (Wash.) of Quantum Chemistry* **2015**, *115*, 1215−1231.
(19) Granucci, G.; Persico, M.; Spighi, G. Surface hopping trajectory simulations with spin-orbit and dynamical couplings. *J. Chem. Phys.* **2012**, *137*, 22A501.
(20) Fedorov, D. A.; Pruitt, S. R.; Keipert, K.; Gordon, M. S.; Varganov, S. A. Ab initio multiple spawning method for intersystem crossing dynamics: Spin-forbidden transitions between 3B1 and 1A1 states of GeH2. *J. Phys. Chem. A* **2016**, *120*, 2911−2919.
(21) Bian, X.; Wu, Y.; Teh, H.-H.; Zhou, Z.; Chen, H.-T.; Subotnik, J. E. Modeling nonadiabatic dynamics with degenerate electronic states, intersystem crossing, and spin separation: A key goal for chemical physics. *J. Chem. Phys.* **2021**, *154*, 110901.
(22) Mead, C. A.; Truhlar, D. G. On the determination of Born-Oppenheimer nuclear motion wave functions including complications due to conical intersections and identical nuclei. *J. Chem. Phys.* **1979**, *70*, 2284−2296.
(23) Berry, M. V. Quantal phase factors accompanying adiabatic changes. *Proc. R. Soc. London A* **1984**, *392*, 45−57.
(24) Berry, M. V.; Robbins, J. Chaotic classical and half-classical adiabatic reactions: geometric magnetism and deterministic friction. *Proc. R. Soc. London. A. Mathematical and Physical Sciences* **1993**, *442*, 659−672.
(25) Fedorov, D. G.; Koseki, S.; Schmidt, M. W.; Gordon, M. S. Spin-orbit coupling in molecules: Chemistry beyond the adiabatic approximation. *Int. Rev. Phys. Chem.* **2003**, *22*, 551−592.
(26) Higuchi, J. Electron Spin−Spin Interaction in Higher Molecular Spin Multiplets. *J. Chem. Phys.* **1963**, *39*, 1847−1852.
(27) Culpitt, T.; Peters, L. D.; Tellgren, E. I.; Helgaker, T. Ab initio molecular dynamics with screened Lorentz forces. I. Calculation and atomic charge interpretation of Berry curvature. *J. Chem. Phys.* **2021**, *155*, 024104.
(28) Wu, Y.; Subotnik, J. E. Electronic spin separation induced by nuclear motion near conical intersections. *Nat. Commun.* **2021**, *12*, 700.
(29) Miao, G.; Bellonzi, N.; Subotnik, J. An extension of the fewest switches surface hopping algorithm to complex Hamiltonians and photophysics in magnetic fields: Berry curvature and "magnetic" forces. *J. Chem. Phys.* **2019**, *150*, 124101.
(30) Wu, Y.; Subotnik, J. E. Semiclassical description of nuclear dynamics moving through complex-valued single avoided crossings of two electronic states. *J. Chem. Phys.* **2021**, *154*, 234101.
(31) Bian, X.; Wu, Y.; Teh, H.-H.; Subotnik, J. E. Incorporating Berry Force Effects into the Fewest Switches Surface-Hopping Algorithm: Intersystem Crossing and the Case of Electronic Degeneracy. *J. Chem. Theory Comput.* **2022**, *18*, 2075−2090.
(32) Subotnik, J. E.; Ouyang, W.; Landry, B. R. Can we derive Tully's surface-hopping algorithm from the semiclassical quantum Liouville equation? Almost, but only with decoherence. *J. Chem. Phys.* **2013**, *139*, 214107.
(33) Kapral, R. Surface hopping from the perspective of quantum-classical Liouville dynamics. *Chem. Phys.* **2016**, *481*, 77−83.
(34) Wu, Y.; Bian, X.; Rawlinson, J. I.; Littlejohn, R. G.; Subotnik, J. E. A phase-space semiclassical approach for modeling nonadiabatic nuclear dynamics with electronic spin. *J. Chem. Phys.* **2022**, *157*, 011101.
(35) Naaman, R.; Waldeck, D. H. Chiral-induced spin selectivity effect. *J. Phys. Chem. Lett.* **2012**, *3*, 2178−2187.
(36) Naaman, R.; Paltiel, Y.; Waldeck, D. H. Chiral molecules and the electron spin. *Nature Reviews Chemistry* **2019**, *3*, 250−260.
(37) Das, T. K.; Tassinari, F.; Naaman, R.; Fransson, J. Temperature-Dependent Chiral-Induced Spin Selectivity Effect: Experiments and Theory. *J. Phys. Chem. C* **2022**, *126*, 3257−3264.
(38) Wu, Y.; Miao, G.; Subotnik, J. E. Chemical Reaction Rates for Systems with Spin-Orbit Coupling and an Odd Number of Electrons: Does Berry's Phase Lead to Meaningful Spin-Dependent Nuclear Dynamics for a Two State Crossing? *J. Phys. Chem. A* **2020**, *124*, 7355−7372.
(39) Fransson, J. Vibrational origin of exchange splitting and "chiral-induced spin selectivity. *Phys. Rev. B* **2020**, *102*, 235416.
(40) Teh, H.-H.; Dou, W.; Subotnik, J. E. Spin Polarization through A Molecular Junction Based on Nuclear Berry Curvature Effects. *arXiv preprint arXiv:2111.12815*, 2021.
(41) Fay, T. P.; Limmer, D. T. Origin of Chirality Induced Spin Selectivity in Photoinduced Electron Transfer. *Nano Lett.* **2021**, *21*, 6696−6702.
(42) Evers, F.; Aharony, A.; Bar-Gill, N.; Entin-Wohlman, O.; Hedegård, P.; Hod, O.; Jelinek, P.; Kamieniarz, G.; Lemeshko, M.; Michaeli, K.; et al. Theory of chirality induced spin selectivity: Progress and challenges. *Adv. Mater.* **2022**, *34*, 2106629.
(43) Shenvi, N. Phase-space surface hopping: Nonadiabatic dynamics in a superadiabatic basis. *J. Chem. Phys.* **2009**, *130*, 124117.
(44) Jain, A.; Alguire, E.; Subotnik, J. E. An efficient, augmented surface hopping algorithm that includes decoherence for use in large-scale simulations. *J. Chem. Theory Comput.* **2016**, *12*, 5256−5268.
(45) Yang, S.; Coe, J. D.; Kaduk, B.; Martínez, T. J. An "optimal" spawning algorithm for adaptive basis set expansion in nonadiabatic dynamics. *J. Chem. Phys.* **2009**, *3*, 04B606.
(46) Kosloff, D.; Kosloff, R. A Fourier method solution for the time dependent Schrödinger equation as a tool in molecular dynamics. *J. Comput. Phys.* **1983**, *52*, 35−53.
(47) Jasper, A. W.; Truhlar, D. G. Improved treatment of momentum at classically forbidden electronic transitions in trajectory surface hopping calculations. *Chem. Phys. Lett.* **2003**, *369*, 60−67.
(48) Littlejohn, R. G.; Flynn, W. G. Geometric phases in the asymptotic theory of coupled wave equations. *Phys. Rev. A* **1991**, *44*, 5239.
(49) Weigert, S.; Littlejohn, R. G. Diagonalization of multi-component wave equations with a Born-Oppenheimer example. *Phys. Rev. A* **1993**, *47*, 3506.
(50) Mead, C. A. The "noncrossing" rule for electronic potential energy surfaces: The role of time-reversal invariance. *J. Chem. Phys.* **1979**, *70*, 2276−2283.
(51) Chandran, S. S.; Wu, Y.; Teh, H.-H.; Waldeck, D. H.; Subotnik, J. E. Electron transfer and spin-orbit coupling: Can nuclear motion lead to spin selective rates? *J. Chem. Phys.* **2022**, *156*, 174113.
(52) Bittner, E. R.; Rossky, P. J. Quantum decoherence in mixed quantum-classical systems: Nonadiabatic processes. *J. Chem. Phys.* **1995**, *103*, 8130−8143.
(53) Subotnik, J. E.; Shenvi, N. A new approach to decoherence and momentum rescaling in the surface hopping algorithm. *J. Chem. Phys.* **2011**, *134*, 024105.
(54) Steiner, U. E.; Ulrich, T. Magnetic field effects in chemical kinetics and related phenomena. *Chem. Rev.* **1989**, *89*, 51−147.
(55) Yuan, M.; Song, Z.; Badir, S. O.; Molander, G. A.; Gutierrez, O. On the nature of C (sp3)-C (sp2) bond formation in nickel-catalyzed tertiary radical cross-couplings: a case study of Ni/photoredox catalytic cross-coupling of alkyl radicals and aryl halides. *J. Am. Chem. Soc.* **2020**, *142*, 7225−7234.
(56) Romero, N. A.; Nicewicz, D. A. Organic photoredox catalysis. *Chem. Rev.* **2016**, *116*, 10075−10166.

https://doi.org/10.1021/acs.jpclett.2c01802
J. Phys. Chem. Lett. 2022, 13, 7398−7404